**WHAT MERCURY'S TOPOGRAPHIC RISES TELL US ABOUT THE INTERIOR.** Peter B. James[1] , Sean C. Solomon[1,2], Maria T. Zuber[3], and Roger J. Phillips[4], [1]Lamont-Doherty Earth Observatory, Columbia University, Palisades, NY 10964, USA (peterj@ldeo.columbia.edu); [2]Carnegie Institution of Washington, Washington, DC 20015, USA; [3]Dept. of Earth, Atmospheric and Planetary Sciences, Massachusetts Institute of Technology, Cambridge, MA 02139, USA; [4]Planetary Science Directorate, Southwest Research Institute, Boulder, CO 80302, USA.

**Introduction:** The Mercury Laser Altimeter (MLA) [1] on the MESSENGER spacecraft is mapping topography in Mercury's northern hemisphere and part of the southern hemisphere [2]. Evidence of long-wavelength tilting that postdates Mercury's smooth plains [2,3,4] hints at the existence of internal processes that acted relatively late in the planet's evolution. The *HgM005* gravity field recovered through radio tracking of the MESSENGER spacecraft [5] allows us to explore these processes through a characterization of the mechanisms of topographic compensation. Aided by a joint analysis of gravity and topography data, we will survey the various physical mechanisms that potentially compensate topography.

**Prominent topographic features:** Whereas impact processes shaped much of Mercury's topography, two classes of long-wavelength topography have no clear relation to basin structures: domical swells and quasi-linear rises [2]. The two most clearly identified domical swells are the northern rise, situated in the northern volcanic plains, and the Budh-Sobkou rise (Fig. 1). Both of these rises have widths of ~1000 km and heights of about 1 km. The quasi-linear rises are more loosely classified, but are generally >1000 km long and ~1 km or more in height.

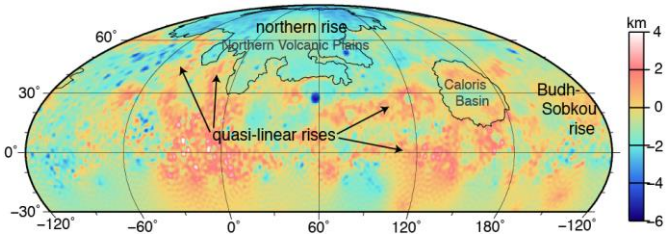


**Figure 1**. Topography on Mercury from MLA. Selected rises and physiographic regions are labeled.

At the relevant spherical harmonic degrees, many of the quasi-linear rises feature low or negative ratios of free air gravity to topography [6] that correspond to apparent compensation depths shallower than the presumed depth of the crust-mantle boundary at ~50 km [7]. Even so, it is likely that these rises are not fully compensated within the crust. The correlations associated with the quasi-linear rises are often much less than unity, so the physical interpretation of associated gravity–topography admittance is complicated. Two or more superimposed compensation mechanisms are likely required to reproduce the observed combination of admittance and correlation values [8].

In contrast to the quasi-linear rises, the domical swells feature high ratios of gravity to topography at long wavelengths and have relatively strong gravity–topography correlations [6]. The domical swells therefore point to the existence of either substantial lithospheric flexure or deep (mantle) compensation.

**A survey of physical compensation mechanisms:** Although flexure of the lithosphere is capable of producing large admittances [9], we disregard flexure as a principal mechanism for supporting long-wavelength topography. Compensation of topography by lithospheric flexure would produce a stress field centered on topographic highs, but no preferred orientation of faulting has yet been observed around the domical swells or quasi-linear rises [10]. Moreover, flexure is expected to support topography at shorter wavelengths [9], whereas dynamic flow preferentially produces topography at the longest wavelengths [11]. We therefore focus on deep support of topography. Below the brittle-ductile transition, deep support of topography comes from mantle dynamic flow, which may exist on Mercury in up to three forms: Rayleigh-Bénard convection, viscous relaxation of perturbed interfaces, or lateral variations in mantle density (Fig. 2).

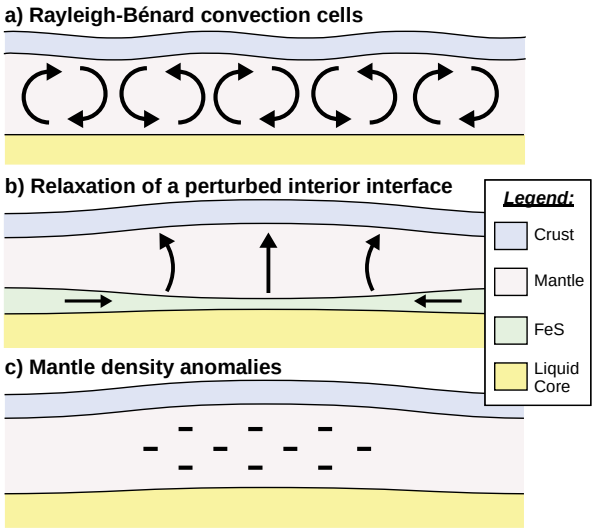


**Figure 2**. Schematic illustration of several physical mechanisms for dynamic topography: (a) Rayleigh-Bénard convection cells, (b) relaxation of a perturbed interior interface, and (c) mantle density anomalies.

*Rayleigh-Bénard convection.* A number of studies have addressed the feasibility of mantle convection throughout Mercury's history [12–14]. We can test whether Rayleigh-Bénard convection is observed on a global scale by plotting the power spectra of crustally-supported topography and dynamic topography as calculated by a dual inversion of gravity and topography [cf. 15]. Whereas convection models predict that dynamic topography should have maximum amplitude at ~350 km length scales (marked by the red arrow; *N. Michel, personal communication*), Fig. 3 shows that the largest amplitudes of dynamic topography appears to come from the longest wavelengths. Thus, we see no evidence for modern convection.

*Relaxation of interior interfaces*. Dynamic topography may also be produced through relaxation of perturbations in a chemically layered interior. Perturbations such as these may be caused by giant impacts or by advectional interaction with the liquid core. In a hypothetical scenario, an FeS layer beneath the mantle that is initially thinned by 10 km may subsequently produce >1 km of surface topography. In order for dynamic topography of this kind to persist over geological time, mantle viscosities must be considerably larger than previously estimated [cf. 6].

*Lateral mantle density variations*. The final potential source of dynamic topography on Mercury is lateral variation in mantle density, in the form of either chemical heterogeneity or residual heating. Chemical heterogeneities are known to have existed in Mercury's early mantle [16], and subsequent heterogeneities may have been introduced through depletion of iron or aluminous phases by partial melting or impact heating [17]. Fig. 4 shows mantle density anomalies between 100 and 300 km depth at Caloris basin, calculated via a dual inversion of gravity and topography [cf. 15].

**Conclusions:** Although it had been predicted that dynamic topography from convection may be distinguishable in gravity and topography [e.g., 12], we do not observe Raylegh-Bénard convection in the MESSENGER data. If convection has in fact ceased, then the Rayleigh number of the mantle can be constrained to $Ra<1100$ for a free-slip lower boundary condition [18]. For a 300-km-thick mantle and a core-mantle boundary temperature of 1800 K, this in turn sets a lower bound of $\eta>2\times10^{22}$ Pa-s for the mantle's viscosity. Other forms of dynamic flow include interior interface relaxation and mantle density heterogeneities; approximately half of Mercury's long-wavelength topography appears to be compensated by one or a combination of these mechanisms. Caloris basin is correlated with a deep-seated buoyancy that is partially masked by crustal thickness variations. This deep-seated buoyancy is comparable in size and amplitude to the buoyant anomalies observed under the northern rise and the Budh-Sobkou rise, giving rise to the possibility that these three regions share similar compensation mechanisms in the mantle.

**References:** [1] Cavanaugh J. F. et al. (2007) *Space Sci. Rev., 131,* 451-479. [2] Zuber M. T. et al. (2012) *Science, 336,* 217-220. [3] Klimczak, C. et al. (2012) *JGR, 117,* E00L03. [4] Balcerski, J. A. et al. (2013) *LPS, 44,* 2444. [5] Srinivasan D. K. et al. (2007) *Space Sci. Rev., 131,* 557-571. [6] James P. B. et al. (2013) *LPS, 44,* abstract 2042. [7] Smith D. E. (2012) *Science, 336,* 214-217. [8] Wieczorek M. A. (2007) *Treatise on Geophysics, 10,* 165-206. [9] Turcotte D. L. et al. (1981) *JGR, 86,* 3951-3959. [10] Klimczak, C. et al. (2012) *JGR, 117,* E00L03. [11] Hager B. H. et al. (1985) *Nature, 313,* 541-545. [12] King S. D. (2008) *Nature Geosci., 1,* 229-232. [13] Tosi N. (2013) *JGR Planets,* 10.1002/jgr3.20168. [14] Michel N. C. et al. (2013) *JGR Planets, 118,* 1033-1044. [15] James P. B. et al. (2013) *JGR Planets, 118,* 859-875. [16] Charlier B. T. et al. (2013) *EPSL, 363,* 50-60. [17] Jordan T. H. (1978) *Nature, 274,* 544-548. [18] Reid W. H. et al. (1958) *Phys. Fluids, 1,* 102-110.

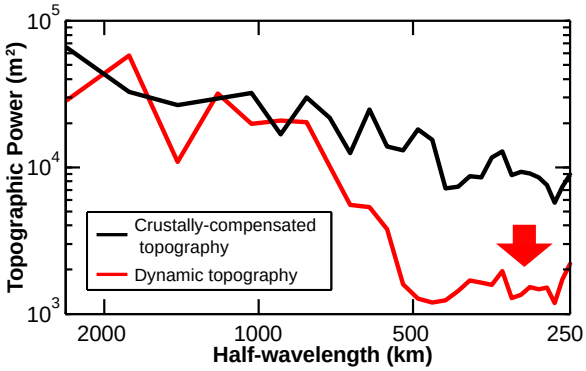


**Figure 3**. Power spectra of crustally-compensated topography and dynamic topography calculated from gravity and topography. The red arrow indicates the predicted length-scale of maximum dynamic topography that would result from modern Rayleigh-Bénard convection.

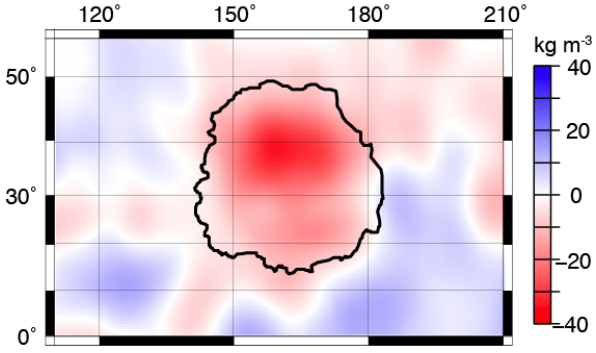


**Figure 4**. Mantle density anomalies in the vicinity of Caloris basin, calculated from a dual inversion of gravity and topography.